Structural characterization of small Xe clusters using their 5*s* correlation satellite electron spectrum

Minna Patanen,† Christophe Nicolas, Xiao-Jing Liu, Oksana Travnikova, and Catalin Miron*

Received Xth XXXXXXXXXX 20XX, Accepted Xth XXXXXXXXX 20XX
First published on the web Xth XXXXXXXXXX 200X
DOI: 10.1039/b000000x

The Xe 5*s* photoelectron spectrum and $5p^4nl$ correlation satellites have been studied in small Xe clusters of an average size of about 15 atoms. The satellite structures are interpreted with the help of the atomic Xe lines. Transition energy shifts between the atomic and the corner/edge/face/bulk components in clusters are divided into polarization screening and exchange interaction energy. Interestingly enough, the ratios between corner/edge/face/bulk polarization screening and exchange interaction energies are found to reflect the ratios of the coordination numbers of corner/edge/face/bulk atoms in these small icosahedral cluster structures.

1 Introduction

The 5*s* photoelectron spectrum of atomic Xe is known to exhibit a rich satellite structure. The first observations of these satellites were made in the 1970's by Gelius[1] using Al Kα radiation, but tunable, high flux synchrotron radiation enabled numerous thorough studies, see *e.g.*[2–5] and references therein. A satisfactory theoretical interpretation for most of the lines was provided by Tulkki[6] using multiconfiguration Dirac-Fock (MCDF) calculations, and it was further supplemented by Lagutin *et al.*[5].

Xe clusters have been intensively studied experimentally in last 10 years. Tchaplyguine *et al.* reported the size-dependent surface-to-bulk intensity ratios in the 4*d* photoelectron spectrum (PES) of small and medium sized Xe clusters[7]. The valence PES of Xe clusters has been studied by Feifel *et al.*, and it was noticed that Xe clusters show a clear indication of band structure formation[8]. Later Lundwall *et al.* studied the 4*d* and the 3*d* PES, as well as the subsequent Auger decay of large Xe clusters, and found different atom-cluster binding energy shifts for the 3*d* and the 4*d* levels[9]. Recently, angular distributions of photoelectrons emitted from clusters have been also studied, for example by Zhang *et al.*[10], who measured the angular distributions of inner-shell 4*d* photoelectrons from Xe clusters. It was found that the angular distributions of inner-shell photoelectrons from the cluster and the free atom are very similar, except for the first 10-15 eV above the photoionization thresholds, where the cluster lines showed less anisotropy than atomic lines.

Synchrotron SOLEIL, L'Orme des Merisiers, Saint-Aubin, BP 48, 91192 Gif-sur-Yvette Cedex, France
†*patanen@synchrotron-soleil.fr*
**Corresponding author: miron@synchrotron-soleil.fr*

Different coordination of surface and bulk atoms in a cluster cause their corresponding photolines or absorption energies to be shifted. This site selective shift was studied by Hatsui *et al.*[11] in different sizes of small Kr clusters. They were able to identify dimer, corner, edge, and face/bulk components in the Kr 3*d* photoelectron spectra for clusters with average sizes of 4, 12, 18, and 30 atoms. The surface-to-bulk energy shift was also a tool used to investigate the Kr and Xe doped Ar clusters[12]. It was found that when the host Ar clusters are doped with Xe, the latter preferentially stays on the surface of the cluster, in contrast to the mixed cluster production by simultaneous co-expansion of the atomic gas mixture.

Recently, Nagasaka *et al.* studied the X-ray absorption spectra of small ($< N > = 15$) Xe clusters[13]. They were able to experimentally estimate the exchange interaction energy between the excited Rydberg electron and the surrounding atoms for various excitation energies and different sites in a cluster. This information was compared to the nearest-neighbor number of an atom sitting on various sites of the cluster, and they concluded that the geometrical structure of small Xe clusters is a mixture of fcc-like cubic and icosahedron-like spherical structures.

Previously, correlation satellites in clusters have been studied by Joshi *et al.*[14]. They recorded the Ne 2*s* PES lines and their correlation satellites for various cluster sizes, and neither a significant energy shift with respect to the atomic lines nor a surface-bulk shift for the low binding energy $2p^4(^1D)3s$ satellite line have been observed.

In this study the 5*s* PES with the $5p^4nl$ correlation satellites is reported for small ($< N > \approx 15$) Xe clusters. Even though formation of the valence band structure has been identified in Xe clusters before[8], the satellite lines studied here show sharper peak structures. The cluster satellite fea-

tures are interpreted with the help of the atomic Xe spectrum. Following the formalism introduced by Nagasaka *et al.*[13], the transition energy shifts between the atomic and the corner/edge/face/bulk components in the clusters are divided into polarization screening and exchange interaction energy. For the studied final state configurations $5p^4nl$, nl=$5d, 6s, 6p$, the ratios between exchange interaction energies are found to reflect the ratios of the coordination numbers of the corner/edge/face/bulk atoms for these small clusters with icosahedral structure. This observation offers an interesting new method to characterize the structure of clusters based on a conventional electron spectroscopy measurement.

2 Experiments and data analysis

The experiment was carried out at the PLEIADES beamline[15–19] at SOLEIL national synchrotron radiation (SR) facility in Saint-Aubin, France. The beamline has two quasi-periodic undulators, HU256 and HU80, which together cover the energy range of 7-1000 eV. In this experiment, the x-ray source was the electromagnetic HU256 (256 mm period) operated in anharmonic mode in order to reduce the amount of higher order radiation. The Xe 5*s* PES was recorded using a 30° wide angle lens VG-Scienta R4000 electron energy analyzer installed on the C-branch of the beamline. The polarization vector of the linearly polarized SR was set parallel to the electron energy analyzer's detection axis. PES were measured using a photon energy of 110 eV, with a monochromator exit slit of 200 μm and a varied line spacing and varied groove depth plane grating with 600 grooves/mm. For the electron energy analyzer, a pass energy of 50 eV and a curved entrance slit of 0.5 mm were used. These settings give a total electron energy resolution of 90 meV. The Xe clusters were produced based on an adiabatic expansion process through a liquid nitrogen cooled nozzle (diameter 0.1 mm, opening angle 2θ=20°). High-purity (99.998%) Xe gas was used as provided by Air Liquide. The cluster source setup is installed in a so-called multi-purpose source chamber (MPSC)[20], which is pumped with two 2700 l/s turbomolecular pumps, ensuring two orders of magnitude pressure difference between the interaction region and the MPSC. The two chambers are separated with a skimmer with a hole of 0.4 mm by Beam Dynamics, Inc. Peltier elements were attached to the nozzle in order to be able to stabilize its temperature to -95°C. Backing pressure was kept at 0.6 bar. From these settings, an average size of $< N > \approx 15$ can be estimated for the produced Xe clusters using the formalism by Buck *et al.*[21]. The neutral clusters were not size-selected and their size distribution is expected to be large. In the same conditions the 4*d* PES (not shown here) clearly exhibits two distinct peaks assigned to "surface" (involving corner and edge atoms) and "bulk" (involving face and bulk atoms) components. The surface component is more intense, which supports the presumed small size of our clusters, but the presence of the "bulk" components shows the existence of larger sizes, involving atoms with higher coordination. Energy calibration was made using atomic photoelectron and satellite lines from the uncondensed Xe, based on the values from the study of Lagutin *et al.*[5] and Kikas *et al.*[22]. PES were fitted using the Igor Pro data analysis software with the curve fitting macro package SPANCF by Kukk[23].

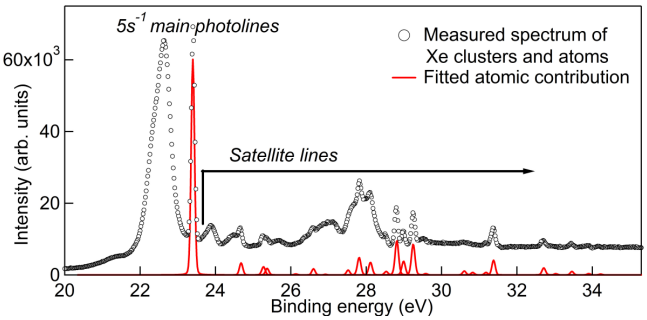

Fig. 1 Experimental 5*s* PES with $5p^4nl$ correlation satellites measured with a photon energy of 110 eV. Circles: signal from both Xe clusters and uncondensed Xe atoms. Solid line: atomic Xe components of the fitted spectrum.

Figure 1 presents the measured 5*s* PES with correlation satellites from Xe clusters and uncondensed Xe atoms. In order to assign the cluster spectral features, the atomic lines were fitted to the spectrum using energies and initial guesses for intensities from the study of Lagutin *et al.*[5]. Figure 2 shows the detail of the fit of the spectrum presented with circles in Fig. 1. During the curve fitting procedure, the relative energy difference within a same group of transitions associated to the same final configuration (same nl in $5p^4nl$ final states) was kept the same as in the atomic Xe. The corner/edge/face/bulk intensity ratio was taken from the fitted $5s^{-1}$ photolines. The main atomic and cluster photolines were modeled by Gaussian lineshapes. The Gaussian linewidths, representing the instrumental broadening and the size distribution, were kept the same and fixed for all the cluster satellite lines. Due to the opening of the ICD channel in the middle of the energy range covered by the studied satellite spectrum (see discussion below), the cluster peaks may have additional Lorentzian broadening as compared to an isolated atom, where the only allowed de-excitation pathway is a fluorescence decay. Thus, a Voigt lineshape was used for the cluster satellite lines. It is clearly seen in Fig. 1 that there is a step-like increase in the background after the first cluster peak. Therefore, a Shirley-type background[24] was used to correct the effect of this stepwise increase in addition to a linear background. As it will be discussed in Section 3, the increase of the background might be due to the electron energy losses by inelastic scatter-

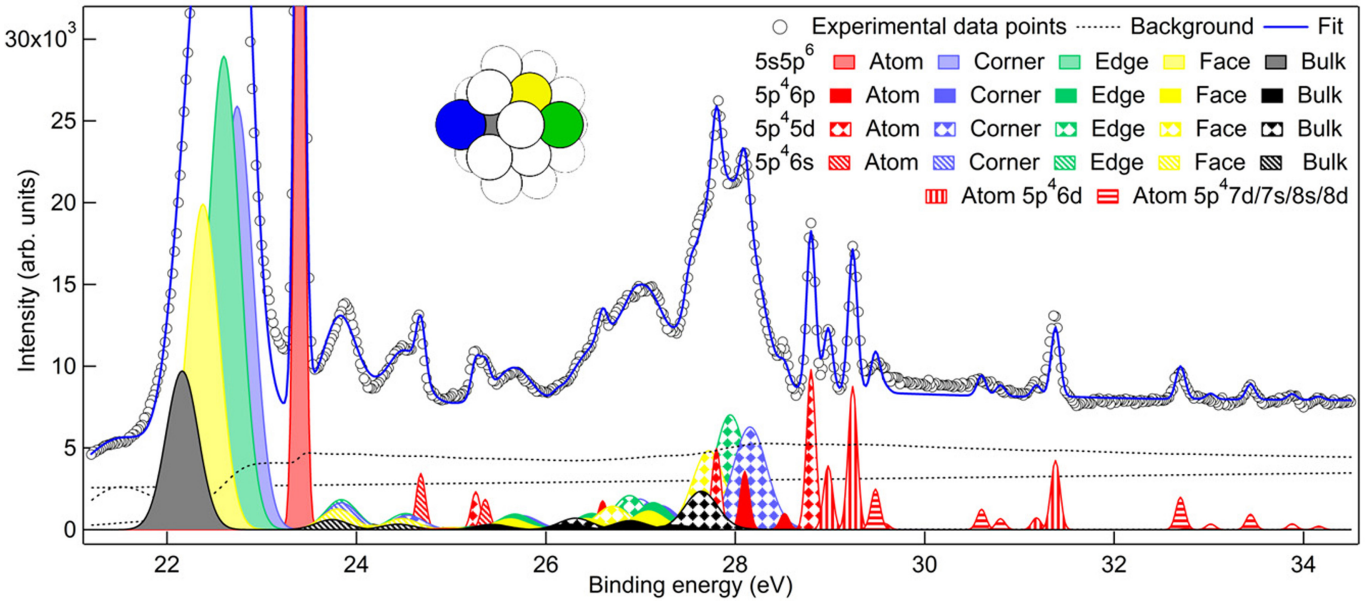

Fig. 2 Fitted $5s^{-1}$ correlation satellite spectrum of Xe clusters and uncondensed atoms. Dashed lines represent three different components of the background, see text for details.

ing, while the ICD transitions mentioned above can also contribute. However, due to the nature of the Shirley background implemented in the fitting program, an artificial increase of the background is seen right after the atomic $5s^{-1}$ photoline, and thus the fit of the very next cluster lines is somewhat disturbed. The broad structure observed before the main photolines was fitted with a broad asymmetric Gaussian in order to gain a reasonable fit of the main lines. While this lower binding energy (higher kinetic energy) prepeak cannot be explained by inelastically scattered 5*s* electrons or ICD processes, from the electron detector image we can clearly see that the electrons associated to this feature are originating from the clusters and not from the uncondensed atoms.

3 Results and discussion

Figure 2 presents the fitted photoelectron spectrum of Xe clusters, the different transitions with the same leading configuration [Kr]$4d^{10}5s^25p^46s$, [Kr]$4d^{10}5s^25p^46p$, and [Kr]$4d^{10}5s^25p^45d$ being coded with different filling patterns while colors refer to different sites in the cluster or to the atomic lines. Table 1 presents the results of the fits: the transition energy differences (ΔE), the final state polarization screening energies ($E_{iPL}(+2)$), and the exchange interaction energies ($E_{EX}(+2)$) derived from the measured Xe cluster satellite spectrum. It also gives the coordination numbers as ratios of the binding energy shift values ($5s^{-1}$ main line) or the exchange interaction energies (excited states). It can be assumed that in the inner-valence ionized states, the only reason for different binding energies between the atom and the clusters is that when an atom is embedded in a cluster, the energy of its final ionized state is lowered due to the polarization screening by the surrounding atoms. Furthermore, in ionized and excited final states, like the $5p^4nl$ satellite states, the surrounding atoms essentially "see" a doubly-charged defect, assuming that the screening effect of the excited electron itself is small. As the polarizability scales as the square of the charge, the polarization screening of the satellite final state can be assumed to be four times the energy difference, ΔE, between the atomic and the corner/edge/face/bulk $5s^{-1}$ photoelectron lines[13]. The excited electron obviously feels the repulsive potential of the electron cloud of the surrounding atoms, introducing an exchange interaction, which adds a "blue-shift" term to the total binding energy shift ΔE. Thus, the exchange interaction energy can be obtained by subtracting $E_{iPL}(+2)$ from ΔE[13]. The exchange interaction energy depends on the nearest neighbors, and by calculating the ratio between $E_{EX}(+2)$ of corner/edge/face/bulk transitions, the ratio between the number of nearest neighbors is achieved. The experimental average ratio 6 : 8 : 11 : 13 is close to the ratio of the coordination numbers of the corner (6 neighbors), edge (8 neighbors), face (9 neighbors), and bulk (12 neighbors) atoms in icosahedral structures. The largest discrepancy is seen in the face component, and it can be argued that every defect in a small cluster effectively decreases the amount of face atoms turning them to edge or corner atoms[11]. The smaller clus-

Table 1 Transition energy differences (ΔE), final state polarization screening energy ($E_{iPL}(+2)$), and exchange interaction energy ($E_{EX}(+2)$) in eV.

Leading config.	ΔE (Cluster - atom)				$E_{iPL}(+2)$				$E_{EX}(+2)$				ratio			
	corner	edge	face	bulk	corner	edge	face	bulk	corner	edge	face	bulk	corner	edge	face	bulk
$5s5p^6$	-0.66±0.05	-0.80±0.05	-1.01±0.05	-1.24±0.10									7^a	8^a	10^a	12^a
$5p^4 6s$	-0.8	-0.8	-0.9	-0.9	-2.62	-3.19	-4.04	-4.94	1.8±0.1	2.4±0.1	3.2±0.2	4.0±0.2	6^b	8^b	11^b	13^b
$5p^4 5d$	-0.7	-0.9	-1.0	-1.2	-2.62	-3.19	-4.04	-4.94	2.0±0.1	2.3±0.1	3.0±0.1	3.8±0.2	7^b	8^b	10^b	13^b
$5p^4 6p$	-0.9	-1.0	-1.0	-1.2	-2.62	-3.19	-4.04	-4.94	1.7±0.2	2.2±0.2	3.0±0.2	3.7±0.2	6^b	8^b	11^b	13^b

[a] Ratio of ΔE(Cluster - atom) values, calculated by setting the value of edge to 8.
[b] Ratio of $E_{EX}(+2)$ values, calculated by setting the value of edge to 8.

ter sizes, also present in the cluster beam, do not have bulk atoms, thus the intensity from the bulk atoms is rather small. These facts are reflected into the uncertainty of the coordination numbers for the face and bulk components. Let us point out that the clusters were produced in a supersonic expansion without size-selection, and the cluster beam contains a large variety of different sizes, which can also have different structures. However, our results are in line with the theoretical studies reporting the icosahedral structure to lead to a global minimum for small clusters described by Lennard-Jones potentials[25]. The electron diffraction studies of small Ar clusters by Farges *et al.*[26] also indicate a polyicosahedral structure, but van de Waal pointed out in his theoretical study[27] that defect-fcc rare gas clusters cannot be ruled out, especially when their bulk form has an fcc crystal structure.

The intensity ratios of the $5s^{-1}$ photolines are approximately 5 : 6 : 4 : 2 (corner : edge : face : bulk). Recently it has been shown for polyatomic gas-phase molecules[28] that partial core-shell photoionization cross-section ratios exhibit EXAFS-like oscillations as a function of the photoelectron energy due to the electron diffraction on surrounding centers, and can therefore be used as a tool for structure determination. This requires the spectra to be recorded as a function of the photon energy several hundred eVs above the photoionization threshold, and since the photoelectron intensity variations can be significant due to the scattering effects[29], we cannot deduce any structural information about the cluster from the intensities by recording the spectrum at a single photon energy.

In order to give a rough description of the different exchange interaction energies in different configurations, it is useful to estimate the overlap between the excited Xe atom in the cluster with its non-excited neighbor atoms. Figure 3 presents the radial density functions (as the square of the large component $P(r)$) of the excited Xe atom (nucleus located at 0 a.u.) and ground state Xe atom (nucleus located at 8.17 a.u.[13]). The wavefunctions for the atomic orbitals were calculated using a relativistic *ab initio* MCDF method utilizing the GRASP92 code[30]. It can be seen that the $5d$ orbital is more contracted than the $6s$ (expectation values of $\hat{r}$ are 3.84,

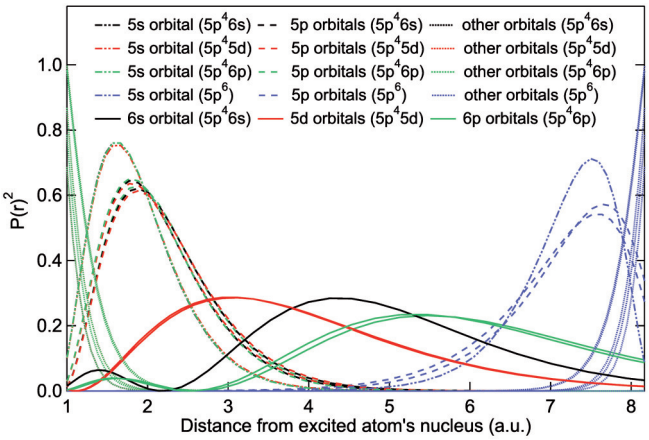

Fig. 3 Squared large component $P(r)$ of the radial wave functions of the excited Xe atom (nucleus located at 0 a.u.) and ground state Xe atom (nucleus located at 8.17 a.u.).

3.88, and 4.87 a.u. for $5d_{3/2}$, $5d_{1/2}$, and $6s_{1/2}$ orbitals, respectively) and thus the overlap between the neighboring atoms is smaller, leading to a smaller exchange interaction. This is consistent with the observed exchange interactions of edge, face, and bulk components tabulated in Tab. 1. The most extended orbital being $6p$ ($\langle\hat{r}\rangle$ is 5.95 and 6.10 a.u. for $6p_{1/2}$ and $6p_{3/2}$ orbitals, respectively), the satellite states involving this orbital, such as $5p^4 6p$, should exhibit the largest exchange interaction energies. This is not observed in our case, partly because the $5p^4 6p$ are the weakest lines and thus the fitting method is not sensitive enough to disentangle these weak transitions from the heavily overlapping structures. In the case of $5p^4 6s$ and $5p^4 5d$ transitions we have three separate somewhat well distinguished structures (the first satellite structure ($5p^4 6s$ leading configuration) and the two strongest structures ($5p^4 5d$ leading configuration) and the analysis is more reliable. One has to also bear in mind that the atomic states are strongly mixed via configuration interaction. For example, the strongest transition to the final state with $5p^4 5d$ leading configuration has a significant component of $5p^4 6d$ configuration,

whereas the states with $5p^4 6s$ and $5p^4 6p$ leading configurations are somewhat more pure[5]. Due to the configuration interaction, the simple relation between the orbital radii and the exchange interaction energy is just a simple qualitative model. For a better description of the orbital overlap it would be necessary to consider also the angular part. In the literature there are two interpretations for the atomic satellite at 27.88 eV (line 10 in[5]). Lagutin *et al.* suggest that it is better described by the $5p^4 6s$ leading configuration, whereas other studies such as Kikas *et al.* label it as $5p^4 5d$. Our analysis indicates that the cluster satellite lines are better fitted in a scheme where this satellite has the same binding energy shift as the strongest $5p^4 5d$ satellite (line 13 in[5]).

One noteworthy aspect is that there do not seem to be cluster satellites above 30 eV. The double ionization potential of clusters can be estimated to be 33.10 eV – 2.7/3.2/4.0/4.8 eV = 30.5/29.9/29.1/28.2 eV, *i.e.* the double ionization of the Xe atom + the polarization screening of the doubly charged final state of corner/edge/face/bulk atoms[13]. By using simple atomic energetics, it can be estimated that an electronic decay of the type: $Xe^+(5p^4nl)$ + $Xe(5p^6) \rightarrow Xe^+(5p^5)$ + $Xe^+(5p^5) + e^-$ is energetically allowed above the binding energy of 24.3 eV of the $Xe^+(5p^4nl)$ states. This transition can be classified as Interatomic Coulombic Decay (ICD), which is known to be a very favorable decay channel in weakly bound systems[31], and its appearance in Xe dimers has been experimentally observed at 27.1 eV by Lablanquie *et al.*[32]. If similar transitions take place in Xe clusters, they might be a plausible explanation for the increased background after the lowest binding energy satellite group, which is seen in Fig. 2 quite clearly around 25-26 eV. This cannot, however, explain the increase of the background before the main photolines, reason for this remains unclear. The cluster Xe $5p^4nl$ satellite peaks are atomic-like in the sense that they have small linewidths as compared to the wide band structure of the $5p$ level. It has been shown that the $4d^{-1}5s^2 5p^6 \rightarrow 4d^{10}5s^2 5p^4$ Normal Auger transitions in clusters lead to Auger lines that can be fitted with the broadened and shifted atomic spectrum[9]. It can be concluded that the doubly ionized final states rather show a more discrete energy level structure than a broader band structure.

Let us point out that the two first satellite structures associated to the $5p^4 6s$ and $5p^4 5d$ configurations have sharper linewidths than other satellite structures, and the peaks are almost superimposed on top of each other without a considerable shift between different ionized sites being noticed. A similar observation was done in the case of the corresponding $2p^4 3s$ satellite line in Ne[14]. In our curve fitting procedure, it was found that these first structures are fitted satisfactorily by constraining the linewidth to the same values as for the main $5s^{-1}$ line. However, the other structures were better fitted with an additional Lorentzian broadening of 40 meV. The corresponding lifetime of 16 fs indicates the existence of an additional decay channel much faster than fluorescence, such as the ICD[33]. However, the above lifetime is only for guidance due to the difficult numerical treatment of the strong background, which could be reproduced by a stronger Lorentzian contribution to the used Voigt profile.

This increased background observed after the cluster peaks might be also due to the inelastically scattered electrons inside the clusters, but a similar behavior of the background was not observed in the $4d$ PES measured in the same conditions. The electron escape depth for 80 eV electrons in Xe is about 40 a.u.[7]. This means that according to the typical interatomic distance of 8.17 a.u.[13], the photoelectrons can penetrate the whole cluster, and such large inelastic scattering losses would be surprising in this case.

4 Conclusions

In this work the $5p^4nl$ correlation satellites of Xe $5s$ photoelectron spectrum of small clusters were found to be an interesting tool to investigate their structure. The ratios between corner/edge/face/bulk polarization screening and exchange interaction energies reflect the ratios of the coordination numbers of corner/edge/face/bulk atoms in small icosahedral cluster structures. A simple model based on atomic calculations of radii of the excited atomic orbitals was utilized to qualitatively describe the different exchange interaction of $5p^4nl$ states. The possible opening of ICD decay channels in the middle of the energy range explored is supported by the observation of an additional Lorentzian broadening of the satellite lines.

Acknowledgments

The experiments were performed at SOLEIL Synchrotron (France) at the PLEIADES beamline, during two beamtimes (proposal numbers 99110074 and 20120568). We are grateful to E. Robert for technical assistance and to the SOLEIL staff for stable operation of the equipment and storage ring during the experiments. Safia Benkoula and Egill Antonsson are acknowledged for assistance during the additional data recording suggested by one of the reviewers during the peer review process.

References

1 U. Gelius, *J. Electron Spectrosc. Rel. Phenom.*, 1974, **5**, 984–1057.
2 M. Y. Adam, F. Wuilleumier, N. Sander, V. Schmidt, and G. Wendin, *J. Physique*, 1978, **39**, 129–135.

3 M. O. Krause, S. B. Whitfield, C. D. Baldwell, J.-Z. Wu, P. van der Meulen, C. A. de Lange, and R. W. C. Hansen, *J. Electron Spectrosc. Relat. Phenom.*, 1992, **58**, 79–104.
4 S. B. Whitfield, B. Langer, J. Viefhaus, R. Wehlitz, N. Berrah, and U. Becker, *J. Phys. B: At. Mol. Opt. Phys.*, 1994, **27**, L359–L366.
5 B. M. Lagutin, I. D. Petrov, V. L. Sukhorov, S. B. Whitfield, B. Langer, J. Viefhaus, R. Wehlitz, N. Berrah, W. Mahler, and U. Becker *J. Phys. B: At. Mol. Opt. Phys.*, 1996, **29**, 937–976.
6 J. Tulkki, *Phys. Rev. Lett.*, 1989, **62**, 2817–2820.
7 M. Tchaplyguine, R. R. Marinho, M. Gisselbrecht, J. Schulz, N. Mårtensson, S. L. Sorensen, A. Naves de Brito, R. Feifel, G. Öhrwall, M. Lundwall, S. Svensson, and O. Björneholm, *J. Chem. Phys.*, 2004, **120**, 345–356.
8 R. Feifel, M. Tchaplyguine, G. Öhrwall, M. Salonen, R. R. T. Marinho, M. Gisselbrecht, S. L. Sorensen, A. Naves de Brito, L. Karlsson, N. Mårtensson, S. Svensson, and O. Björneholm, *Eur. Phys. J. D*, 2004, **30**, 343.
9 M. Lundwall, R. F. Fink, M. Tchaplyguine, A. Lindblad, G. Öhrwall, H. Bergersen, S. Peredkov, T. Rander, S. Svensson, and O. Björneholm, *J. Phys. B: At. Mol. Opt. Phys.*, 2006, **39**, 5225–5235.
10 H. Zhang, D. Rolles, Z. D. Pešic, J. D. Bozek, and N. Berrah, *Phys. Rev. A*, 2008, **78**, 063201.
11 T. Hatsui, H. Setoyama, N. Kosugi, B. Wassermann, I. L. Bradeanu, and E. Rühl, *J. Chem. Phys.*, 2005, **123**, 154304.
12 A. Lindblad, H. Bergersen, T. Rander, M. Lundwall, G. Öhrwall, M. Tchaplyguine, S. Svensson, and O. Björneholm, *Phys. Chem. Chem. Phys.*, 2006, **8**, 1899–1905.
13 M. Nagasaka, T. Hatsui, H. Setoyama, E. Rühl, and N. Kosugi, *J. Electron Spectrosc. Relat. Phenom.*, 2011, **183**, 29.
14 S. Joshi, S. Barth, S. Marburger, V. Ulrich, and U. Hergenhahn, *Phys. Rev. B*, 2006, **73**, 235404.
15 C. Miron *et al.*, http://www.synchrotron-soleil.fr/Recherche/LignesLumiere/PLEIADES
16 O. Travnikova, J. C. Liu, A. Lindblad, C. Nicolas, J. Söderström, V. Kimberg, F. Gel'mukhanov, and C. Miron, *Phys. Rev. Lett.*, 2010, **105**, 233001.
17 J. Söderström, A. Lindblad, A. Grum-Grzhimailo, O. Travnikova, C. Nicolas, S. Svensson, and C. Miron, *New J. Phys.*, 2011, **13**, 073014.
18 C. Miron, C. Nicolas, O. Travnikova, P. Morin, Y. P. Sun, F. Gel'mukhanov, N. Kosugi, and V. Kimberg, *Nature Phys.*, 2012, **8**, 135–138.
19 A. Lindblad, V. Kimberg, J. Söderström, C. Nicolas, O. Travnikova, N. Kosugi, F. Gel'mukhanov, and C. Miron, *New J. Phys.*, 2012, **14**, 113018.
20 A. Lindblad, J. Söderström, C. Nicolas, E. Robert, and C. Miron, submitted to *Rev. Sci. Instrum.* (2013).
21 U. Buck and R. Krohne, *J. Chem. Phys.*, 1996, **105**, 5408.
22 A. Kikas, S. J. Osborne, A. Ausmees, S. Svensson, O.-P. Sairanen, and S. Aksela, *J. Electron Spectrosc. Relat. Phenom.*, 1996, **77**, 241–266.
23 E. Kukk, Spectral Analysis by Curve Fitting Macro Package /SPANCF/ 2000 - http://www.physics.utu.fi/en/department/materials_research/materials_science/Fitting.html
24 J. Végh *J. Electron Spectrosc. Relat. Phenom.*, 2006, **151**, 159.
25 D. J. Wales and J. P. K. Doye, *J. Phys. Chem. A*, 1997, **101**, 5111–5116.
26 J. Farges, M. F. de Feraudy, B. Raoult, and G. Torchet, *J. Chem. Phys.*, 1983, **78**, 5067–5080.
27 B. W. van de Waal, *J. Chem. Phys.*, 1992, **98**, 4909–4919.
28 E. Plésiat, L. Argenti, E. Kukk, C. Miron, K. Ueda, P. Decleva, and F. Martín, *Phys. Rev. A*, 2012, **85**, 023409.
29 J. Söderström, N. Mårtensson, O. Travnikova, M. Patanen, C. Miron, L. J. Sæthre, K. J. Børve, J. J. Rehr, J. J. Kas, F. D. Vila, T. D. Thomas, S. Svensson, *Phys. Rev. Lett.*, 2012, **108**, 193005.
30 F. A. Parpia, C. F. Fischer, and I. P. Grant, *Comput. Phys. Comm.*, 1995, **94**, 249.
31 L. S. Cederbaum, J. Zobeley, and F. Tarantelli, *Phys. Rev. Lett.*, 1997, **79**, 4778.
32 P. Lablanquie, T. Aoto, Y. Hikosaka, Y. Morioka, F. Penent, and K. Ito, *J. Chem. Phys.*, 2007, **127**, 154323.
33 G. Öhrwall, M. Tchaplyguine, M. Lundwall, R. Feifel, H. Bergersen, T. Rander, A. Lindblad, J. Schulz, S. Peredkov, S. Barth, S. Marburger, U. Hergenhahn, S. Svensson, and O. Björneholm, *Phys. Rev. Lett.*, 2004, **93**, 173401.